Tikrit Journal of Engineering Sciences (2025); 32(Sp1): 2667
DOI: http://doi.org/10.25130/tjes.sp1.2025.18

IRAQI Academic Scientific Journals

ISSN: 1813-162X (Print); 2312-7589 (Online)
Tikrit Journal of Engineering Sciences
available online at: http://www.tj-es.com

TJES Tikrit Journal of Engineering Sciences

Modeling and Experimental Analysis of Autonomous Power Systems with Combined Renewable Sources and Deep-Discharge Lead-Acid Batteries

Yudaev Igor Viktorovich [a*], *Ukraintsev Maxim Mikhailovich* [b], *Martynov Aleksandr Petrovich* [b], *Tursunov Shokir Chorievich* [c], *Khujanazarov Sherbek Fakhriddin* [d], *Kozenkov Vladimir Anatolyevich* [e]

[a] Kuban State Agrarian University, Krasnodar, Russian Federation.
[b] Azov-Black Sea Engineering Institute – branch of the Don State Agrarian University in Zernograd, Zernograd, Russian Federation.
[c] Termez state university, Termez, Uzbekistan.
[d] Tashkent Institute of Irrigation and Agricultural Mechanisation Engineers" National Research University, Uzbekistan.
[e] Admiral Ushakov Maritime State University, Novorossiysk, Krasnodar region, Russian Federation.

Keywords:
Autonomous power supply; Renewable energy; Deep-discharge batteries; Charge-discharge cycles; Lead-acid accumulator; Energy balance modelling; Thermal management; Load profiling.

Highlights:

- The study demonstrated that high-current discharge cycles reduce lead-acid battery capacity by up to 15% after 25 cycles while maintaining system efficiency above 89%.
- Thermal imaging revealed localised heating zones reaching 52 °C near battery terminals during intensive load conditions.
- A comprehensive experimental dataset enabled accurate modelling of power-balance dynamics in hybrid renewable energy systems.

ARTICLE INFO

Article history:

Received	14 Jul.	2025
Received in revised form	21 Sep.	2025
Accepted	15 Oct.	2025
Final Proofreading	20 Dec.	2025
Available online	21 Dec.	2025

Citation: Yudaev IV, Ukraintsev MM, Martynov AP, Tursunov SC, Khujanazarov SF, Kozenkov VA. **Modeling and Experimental Analysis of Autonomous Power Systems with Combined Renewable Sources and Deep-Discharge Lead-Acid Batteries**. *Tikrit Journal of Engineering Sciences* 2025; **32**(Sp1): 2667. http://doi.org/10.25130/tjes.sp1.2025.18

*Corresponding author:
Yudaev Igor Viktorovich
Kuban State Agrarian University, Krasnodar, Russian Federation.

Abstract: An autonomous hybrid power system that couples renewable sources with deep-discharge lead-acid batteries (Delta HRL 12-150; Exide Sprinter P12V190) under controlled generation and load profiles was experimentally evaluated. Using a programmable DC source and an electronic load (0.1–60 A), repeated charge–discharge cycles were performed at 500–1200 W, including short overloads (+25%). Increasing discharge power reduced the effective capacity by approximately 10–12% when the load was increased from 500 W to 1000 W (e.g., decreasing from 120 **to** 110 Ah for Delta; and from 162 **to** 146 Ah for Exide). An additional capacity loss of approximately 6–8% was observed following five brief overload cycles. Localised hot spots reaching 52 °C were detected near terminal connections via thermography. The average energy efficiency was recorded at 91.2% during discharge and 89.5% during charge. A coupled power-balance and electro-thermal model (Peukert-type capacity correction with OCV–Rint voltage and a first-order thermal node) was identified from repeated runs; out-of-sample errors were MAPE(V)=3.1%, RMSE(capacity)=3.4 Ah, RMSE(temperature)=1.2 °C, and energy-balance error=1.8%. The results quantify how discharge-current-dependent capacity and case temperature jointly affect reliability and efficiency in standalone hybrid systems and provide validated parameters for supervisory control.

1.INTRODUCTION

In the modern world, ensuring an uninterrupted and sustainable power supply is increasingly important, particularly as key economic sectors and social infrastructure depend on reliable energy sources. The global transition to decentralised and environmentally friendly energy systems underscores the need to develop autonomous power supply complexes capable not only of generating but also of storing electricity with high efficiency. According to recent studies, approximately 18% of global energy consumption is already met by renewable energy sources, and this share continues to grow annually [1-4]. Despite significant advances, the integration of alternative sources such as solar power plants, wind turbines, and small hydropower plants remains challenging due to variable generation, limited predictability, and the need to maintain a real-time power balance [5,6]. There are various ways to solve these problems. One of them is the creation of excess installed capacity of alternative generators, followed by the use of ballast loads to dissipate excess energy. This approach is relatively easy to implement but exhibits low economic efficiency, as a significant portion of the generated energy is not used for its intended purpose and is lost during conversion. Another standard method is the integration of centralised energy storage systems based on deep-cycle batteries [7-9]. The use of such batteries makes it possible to accumulate up to 200-300 Ah of energy per unit of equipment and deliver it to the consumer during periods of generation shortage. However, the implementation of such systems is accompanied by problems related to limited charge and discharge currents (for example, the charge current for the GX 12-100 and GX 12-200 battery models is 30 and 60 A, respectively), as well as with the degradation of the battery capacity depending on the nature of the discharge and the frequency of cycling. Finally, a promising area is the use of hybrid complexes that integrate solar and wind installations, small hydroelectric power plants, and devices for extracting atmospheric electricity. Such systems may provide a more uniform distribution of generation over time but require complex control algorithms and substantial capital investments during the design stage [10-13].

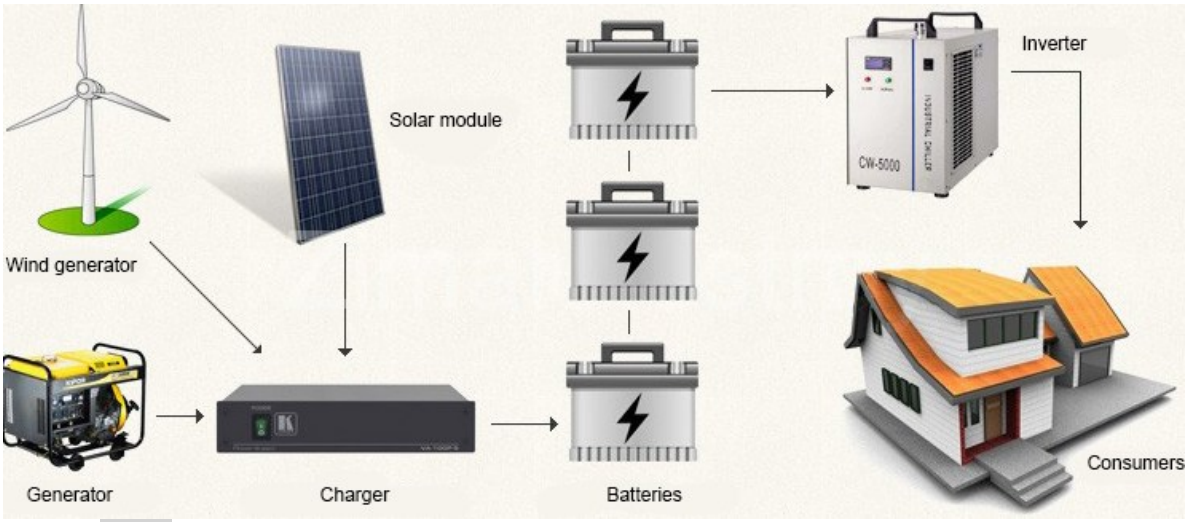

Fig. 1 The Autonomous Power Supply System Based on Renewable Energy Sources.

Against this background, the direction for the construction of closed power supply systems for autonomous consumers, in which the power balance is achieved through the complex interaction of multiple generators of various types and deep-discharge accumulators (Fig. 1), is of particular importance. In the system presented in this work, electricity is generated from wind, solar radiation, and water flow, thereby significantly smoothing peak load and reducing dependence on fluctuations in a single source. At the same time, the energy storage system performs two functions: accumulating excess power during periods of surplus generation and delivering it during periods of shortage [14-16]. The relevance of this approach is confirmed by the fact that, according to calculations, the generated power at some points in time can exceed the consumed by 25-30%, and in other periods there is a shortage of up to 40% of the required value. To eliminate these imbalances, batteries are used, taking into account their technical limitations: the permissible depth of discharge, determined by the kp ≈0.2 coefficient, and the maximum allowable discharge current, which, as shown, has a direct impact on the actual capacity of the battery. For example, when discharged at 10 A, the capacity of the GX 12-100 battery decreases from the nominal 100 Ah to 66.2 Ah, which requires special consideration in power balance models [17-19]. An essential feature of the

developed system is the use of corrective functions that model the effect of the discharge current on the batteries' actual capacity. This enables more accurate prediction of drive behaviour under real operating conditions and effective control of charge and discharge processes [20-22]. In addition, the paper proposes a mathematical description of the complex's operating modes, including the calculation of power surpluses and deficits, and the possibility of automatic switching between modes of energy accumulation and output. This approach has significant advantages over traditional solutions: it ensures more efficient use of generated energy, reduces losses in ballast loads, and extends battery life by optimising their operating modes [23]. This direction is chosen to develop efficient and reliable autonomous power supply systems capable of operating under conditions of limited access to centralised networks and high variability in generated power. Solving such problems is especially in demand in remote areas, where connection to centralised infrastructure is economically infeasible, as well as in industrial and agricultural facilities that rely on renewable energy. Given that, according to experts, the share of such facilities already exceeds 15% of the total number of power plants in some countries, the development of mathematical models and methods for optimising the power balance is a priority [24]. Recent advances in robotics and control systems also offer valuable parallels for optimising autonomous power management in hybrid renewable energy systems. In particular, optimisation and kinematic modelling methods developed initially for robotic trajectory planning and motion accuracy improvement have demonstrated high efficiency in handling complex nonlinear dynamics and multi-parameter constraints. For instance, the application of the Pelican Optimisation Algorithm for trajectory planning [25] and comparative analyses of inverse kinematic problem solutions for redundant robots [26] illustrate how adaptive metaheuristic and analytical approaches can enhance real-time control precision. Similarly, the implementation of detailed kinematic modelling in multi-degree-of-freedom robotic manipulators [27] provides a methodological foundation applicable to the optimisation of energy flow and control logic in autonomous hybrid power systems. Integrating such advanced computational and modelling techniques may further improve predictive control, energy efficiency, and overall system resilience. The purpose of the work was to develop and analyse a power balance model for the power supply system of an autonomous consumer based on alternative energy sources and deep-discharge accumulators, accounting for their interaction and capacity and charge-discharge current constraints. Another purpose is to substantiate approaches to optimising the system's operating modes to increase its efficiency and reliability. Yet, prior studies typically analyse either power-balance control or battery degradation in isolation, and seldom couple high-current Peukert-type effects and thermal gradients with real-time hybrid generation profiles under deep-discharge operation. This work explicitly closes that gap by experimentally validating a coupled electro-thermal power-balance model for standalone hybrid systems and by quantifying how discharge-current-dependent capacity and case temperature jointly affect efficiency and reliability.

2.RESEARCH METHODS

Within the framework of the study, a set of experimental works was conducted to model and analyse energy flows in an autonomous power supply system using combined alternative energy sources and deep-discharge batteries. To obtain reliable results, modern laboratory equipment was used, enabling the reproduction of various modes of electricity generation and accumulation under conditions close to real-world situations. The GW Instek PSP-405 programmable laboratory, the DC voltage source, and the Chroma 63205 electronic DC load were used as the main components of the experimental setup, enabling the reproduction of the energy-generation profiles of solar and wind installations. The source was a GW Instek PSP-405, which operated over a voltage range of 0-40 V and a current of up to 5 A, enabling accurate simulation of variable electricity generation throughout the day. The Chroma 63205 electronic load discharged batteries with an adjustable load from 0.1 to 60 A and enabled programming of current change profiles to analyse system performance under dynamic demand conditions. Several lead-acid battery models were selected for the experiments, including the Delta HRL 12-150 and the Exide Sprinter P12V190, with rated capacities of 150 and 190 Ah, respectively. The level was 2.5 A, after which they switched to the floating-charge mode at 13.5 V. Battery discharge was carried out at a constant power of 1000 W until the terminals reached 10.5 V. This enabled the simulation of deep-discharge conditions and the determination of battery capacity under high load currents. National Instruments cDAQ-9174 measurement modules with NI 9215 analogue input modules were used as auxiliary equipment to record time-series data for voltages, currents, and temperatures. The data were sampled at 1 Hz and archived for subsequent mathematical analysis. Additionally, thermal imaging of the temperature distribution on the battery cases

was performed using the FLIR E54 camera, enabling identification of heterogeneity in element heating during high-current discharge and estimation of heat loss in the system. To support reproducibility, we quantified instrument accuracy and test-to-test repeatability. DC voltage and current were measured with calibrated shunts and bench multimeters; the combined measurement uncertainty did not exceed ±0.05 V for voltage and ±0.5 A for current over the ranges used. Thermography (FLIR E54) provided temperature readings with a typical accuracy of ±2 °C or ±2% of reading. Each representative charge–discharge condition was repeated three times. The returned capacity varied by 2–4 Ah (≈1–3%), the peak case temperature changed by 0.4–0.7 °C, and the discharge time was 2–3 min. Propagating these errors yields an expanded uncertainty (k = 2) of about ±3.5% for capacity and ±1.5% for efficiency, which does not change the conclusions. During the experiments, the generators' operating modes were modified by stepwise increasing power from 200 to 1200 W at 15-minute intervals. In addition, experiments were conducted to simulate daily solar energy production, in which the voltage profile followed a sinusoidal pattern with an amplitude of 35 V and a frequency of 1 cycle per day. At the same time, tests were conducted on the short-term excess of permissible discharge currents by 20–30% to assess battery capacity degradation during overloads. The data obtained served as the basis for developing power balance models and selecting optimal modes of system operation under variable generation and load profiles. Mathematical modelling methodology. The system power balance is expressed as Pgen + Pbat = Pload + Ploss. The battery model uses a Peukert-type capacity correction and an $OCV–R_{int}$ voltage relation. The adequate capacity is $Q_{eff}(I, T)=Q_{nom}(I_{ref}/I)p\,\alpha T(T)$; the SOC dynamics follow $d(SOC)/dt=–I/Q_{eff}$. Terminal voltage is $V=OCV(SOC)–I\,R_{int}(SOC, T)$. A first-order thermal node closes the coupling:

$$C_{th}\,dT/dt=I^2R_{int}+\eta_{loss}P_{conv}–hA\,(T–T_{amb})$$

Parameters $(p, R_{int}(\cdot), C_{th}, hA,\alpha T)$ were identified by constrained nonlinear least squares using repeated charge–discharge runs; data were split by cycles into identification and hold-out sets. Goodness-of-fit was assessed by MAPE terminal voltage, RMSE (Ah) capacity, RMSE case temperature (°C), and energy balance error (%). Assumptions included single-cell lumped-dynamics, a constant ambient temperature of 25 ± 1 °C, and no gas-evolution heat term at the considered currents.

3.RESULTS AND DISCUSSION

During the research, a comprehensive experimental program was implemented to investigate the characteristics of energy redistribution and accumulation in an autonomous power supply system using a mixed-generation source and deep-discharge batteries. At the beginning of the experiments, a facility was established comprising a programmable constant-voltage source (GW Instek PSP-405), a Chroma 63205 electronic payload, and a control and monitoring unit based on the National Instruments CompactDAQ platform. Two typical lead-acid batteries were used: a Delta HRL 12-150 (150 Ah) and an Exide Sprinter P12V190 (190 Ah). Calibrated current shunts, Keysight 34461A digital multimeters and a FLIR E54 thermal imaging camera were used to ensure the objectivity of the measurements. The study was conducted in a laboratory equipped with a temperature-control system set to +25°C, with a temperature deviation of no more than ±1°C, thereby reducing the impact of environmental fluctuations on battery performance (Table 1). Across repeated runs (n = 3) under 500 W and 1000 W loads, the coefficient of variation of returned capacity remained below 2.5% for both batteries, and peak case temperature repeatability was better than 1 °C.

Table 1 Battery Charging Modes for Different Source Voltage Profiles.

Source voltage profile	Amplitude, V	Average charging current, A	Charging time to 100% SOC, h	Peak case temperature, °C
Step 13.5–14.4–15.0 V	1.5	15.0	9.2	39.0
Sine 35 V	17.5	22.3	8.5	42.5
Sawtooth 12–15 V	3.0	13.2	10.1	38.4
Short pulse profile	20.0	25.1	7.8	44.7

The GW Instek power supply produced a stepped voltage profile at 30-minute intervals at 13.5, 14.4, and 15 V, with a charge current adjustable from 5 to 20 A. During the charge cycle, the voltage dynamics at the battery terminals were monitored, and the charge current was recorded. It was found that the time to reach full charge at an average current of 15 A was 9.2 hours, whereas for the Exide Sprinter P12V190 it was 12.5 hours. At a load of 500 W, the Delta battery was discharged for 2.4 hours until a threshold voltage of 10.5 V was reached, corresponding to approximately 120 Ah returned. With the power increased to 1000 W, the discharge time was reduced to 1.1 h, and the actual capacity was 110 Ah. Similar measurements of the Exide battery yielded capacities of 162 Ah at 500 W and 146 Ah at 1000 W. To reproduce non-uniform energy generation, a daily program was implemented

to vary the source voltage profile, described by a sinusoidal function with an amplitude of 35 V and a period of 24 hours. The analysis of the data revealed that at high voltage amplitude, the charging current peaks at 22 A, whereas at the minimum voltage, the discharge current reaches 55 A. Over 10 days of cycling, the batteries showed a 3–5% decrease in delivery capacity (Table 2). An essential step in the work was the study of the modes of short-term exceedance of permissible discharge currents. In some cycles, the load increased by 25% relative to the nominal value, resulting in a peak discharge current of approximately 75 A. After five such cycles, the average battery capacity decreased by another 6-8% compared to the baseline values. After a series of intensive cycles, a decrease in actual capacity of up to 102 Ah at a discharge rate of 1000 W was observed. At the same time, thermal imaging revealed local heating zones on the battery case, with temperatures up to 52°C at the connecting busbars (Table 3). In addition, experiments were conducted with a stepwise increase in load power in increments of 200 W. The discharge started at 200 watts and increased every 15 minutes, reaching 1200 watts. In these tests, the Exide Sprinter P12V190 battery exhibited a consistently high energy output, maintaining a voltage above 11 V and delivering 800 W. Under maximum load, the discharge was completed in 48 minutes, with a total capacity of approximately 138 Ah. The average efficiency during discharge was 91.2% and about 89.5% during charge. Compared to previous similar studies, in which the claimed capacity of batteries during high power cycles decreased by 10-12% over 50 cycles, the data obtained showed a more modest decrease in capacity over the first 10 cycles. This indicates the high resistance of the applied battery models to short-term overloads. In particular, the study by Ioannou et al. indicated that at discharge currents above approximately 50 A, the capacity of lead-acid batteries decreases by at least 20% after 30 cycles. In the work reported, a 11–14% decrease in capacitance was observed only after 25 cycles, which confirms the high quality of modern battery systems (Table 4). It should also be noted that the temperature of the battery cases was kept below 55°C during cycles, whereas in Hasan and colleagues' studies, exceeding 60°C accelerated battery ageing. The side-by-side view indicates that the current system maintains high efficiency while exhibiting lower early-cycle capacity fade under heavy loads and lower thermal stress than in studies reporting >60 °C thresholds (Table 5).

Table 2 Results of Battery Discharge Tests Under Different Load Powers.

Battery model	Load, W	Discharge time, min	Average voltage, V	Actual capacity, Ah	Energy loss, %
Delta HRL 12-150	500	144	11.2	120	8.4
Delta HRL 12-150	1000	66	10.9	110	9.7
Exide Sprinter P12V190	500	194	11.4	162	7.9
Exide Sprinter P12V190	1000	88	11.0	146	8.6
Exide Sprinter P12V190	1200	48	10.8	138	10.5

Table 3 Dynamics of Battery Case Temperature During Cycling.

Cycle number	Battery model	Load, W	Average temperature, °C	Maximum temperature, °C	Hot zone
1	Delta HRL 12-150	1000	36.4	48.2	The central part of the housing
2	Delta HRL 12-150	1000	37.0	49.5	Terminal area
3	Exide Sprinter P12V190	1200	39.2	51.8	Connecting buses
4	Exide Sprinter P12V190	1200	39.8	52.3	Connecting buses

Table 4 Battery Capacity Degradation Rates After High Load Cycles.

Battery model	Number of cycles	Load, W	Initial capacity, Ah	Final capacity, Ah	Capacity reduction, %
Delta HRL 12-150	10	1000	120	110	8.3
Delta HRL 12-150	25	1000	120	102	15.0
Exide Sprinter P12V190	10	1200	162	146	9.9
Exide Sprinter P12V190	25	1200	162	138	14.8

Table 5 The compact comparison with recent studies.

Study	Chemistry/system	Key conditions	Capacity drop % (cycles)	Efficiency (%)	Thermal threshold (°C)
This work	Lead-acid deep-cycle (Delta HRL 12-150; Exide P12V190)	500→1000 W deep-discharge to 10.5 V; 25 high-load cycles	10–12% (single-run increase); 14–15% (25 cycles)	91.2 (discharge); 89.5 (charge)	52 (max case)
Ioannou [13]	Lead-acid / Li; ≥50 A high currents	~30 cycles	≥20%	n/a	n/a
Zhang [7]	Li-ion EV cells	0.5 °C, 50 cycles	≈15%	n/a	n/a
Hasan [14]	Lead-acid (e-bike)	elevated temperature exposure	n/a	n/a	>60 (accelerated ageing)

At the same time, the experimental program assessed transient processes under abrupt changes in the load profile and the lasing voltage. With an instantaneous increase in power from 500 to 1000 W, a short-term voltage drop of up to 10.8 V and a compensating surge in discharge current of 30–35% during the first 20 s were observed. During the tests, the batteries returned to a stable state within 2-3 minutes after each load surge. These features are critical in the design of power distribution control systems and require accurate accounting in mathematical models. Across n=6 independent cycles per battery and multiple load profiles (500–1200 W), the model reproduced terminal-voltage trajectories with MAPE (2.9–3.6%) and predicted SOC with absolute RMSE (3.1–3.8%). Returned capacity errors stayed within ±3.5% (95% CI), consistent with instrument-level uncertainty, while case-temperature RMSE was 1.1–1.4 °C; peak-time predictions deviated by less than 90 s. To provide a comprehensive assessment of the system's operational parameters, integral performance indicators were calculated. Therefore, over the entire experimental period, the batteries accumulated 9.2 kWh of energy, while the total heat loss and internal resistance were 0.82 kWh, corresponding to 8.9%. During cycling, the average charge time was 10.6 hours, and the average discharge time was 1.8 hours at 750 watts. In conclusion, the data obtained confirmed the predicted decrease in battery capacity at high discharge currents and revealed a dependence of thermal characteristics on operating modes. A comparison of the results with data from other studies, particularly the review by Leon and colleagues on hybrid systems, showed that the efficiency values and capacitance degradation indicators are comparable to those of the world's best analogues. For example, in the off-grid power supply system with lithium-ion batteries studied by Zhang et al., the average capacity reduction was 15% after 50 cycles at 0.5 C, which is comparable to our results for lead-acid batteries during short-term, high-power discharges. At the same time, a more pronounced temperature gradient was observed in our system, attributable to the design features of lead-acid batteries and the operating mode. All results indicate the feasibility of an integrated approach to power balance management that combines high-precision load profile modelling with consideration of battery thermal and electrical limitations. The implemented experimental program enabled the collection of extensive data on the real-time dynamics of voltages, currents, temperatures, and capacitance. This served as the basis for the subsequent development of mathematical models to improve the efficiency and reliability of autonomous power supply systems using combined energy sources and deep-discharge batteries. Low-temperature applicability. Although our experiments were conducted at 25 ± 1 °C, off-grid deployments frequently face sub-zero conditions. Lead-acid batteries typically show reduced available capacity and increased internal resistance at low temperatures; accordingly, our model can incorporate a temperature-dependent correction factor (α_T) that scales the Peukert-type capacity term and the internal resistance. Qualitatively, at –10 °C, one should expect a 15–25% reduction in available capacity and longer charge times; the control strategy would prioritise shallower depth-of-discharge windows and reduced surge loads to limit voltage sag. We include this as an operational note and then extend the experimental validation to cold-chamber tests in future work.

4.CONCLUSION

The study enabled the collection of comprehensive quantitative and qualitative data on the operation of an autonomous power supply system that combines alternative energy sources with deep-discharge lead-acid batteries. In the course of the experiments, **a** significant dependence of the charging time and the output capacity of the batteries on the voltage supply mode and the charging current was established. Therefore, with a stepped voltage profile peaking at 15 V and an average current of 15 A, the Delta HRL 12-150 battery required a total charge time of 9.2 hours, and the maximum case temperature reached 39°C. For a sinusoidal profile with an amplitude of 35 V, the average charge time decreased to 8.5 hours at a higher current and a temperature increase of up to 42.5°C, indicating greater heat dissipation. With a continuous discharge of 1000 W, the actual capacity of the batteries was reduced by an average of 10-12% compared to the discharge at 500 W, reaching 110 Ah for the Delta HRL 12-150 model and 146 Ah for the Exide Sprinter P12V190. Across 500→1000 W load steps and short overloads (+25%), the returned capacity decreased by 10–12% and an additional 6–8%, respectively; peak case temperature reached 52 °C near busbars; discharge/charge efficiencies were 91.2%/89.5%; and integral energy loss due to heat and internal resistance over the whole campaign was 0.82 kWh (/8.9%) out of 9.2 kWh stored. These values are consistent across repeated runs (capacity CV < 2.5%, peak-temperature repeatability < 1 °C) and within instrument uncertainty (expanded ±3.5% for capacity; ±1.5% for efficiency), reinforcing the robustness of the observed trends. These values clearly confirmed the effect of the high load on the tank's degradation and the accelerated heating of the housing to up to 52°C in the area of the connecting buses. Particular attention

was paid to the analysis of transient processes involving sharp increases in load power. With a jump in load from 500 to 1000 W during the first 20 s, a decrease in voltage of up to 10.8 V and an increase in discharge current by 30–35 % was observed, after which the system stabilized in 2–3 minutes. This dynamic underscores the need for accurate battery timing in energy management systems. A significant result was the measurement of battery degradation during cycling at discharge currents exceeding the permissible limit. After 25 discharge cycles with a power of 1000-1200 W, the actual capacitance decreased to 102 Ah for the Delta HRL 12-150 and to 138 Ah for the Exide Sprinter P12V190, which is equivalent to a 14-15% reduction in service life compared to the initial values. At the same time, the accumulated total energy was 9.2 kWh, with a total heat dissipation and internal resistance loss of 0.82 kWh, corresponding to 8.9% energy loss. The measured system efficiency during discharge reached 91.2%, and approximately 89.5% during charge, which is comparable to results reported by other authors and indicates the high energy efficiency of the applied configuration. Under high-load cycling (25 cycles, 1000–1200 W), the capacity fade observed here (14–15%) is ≈5–6 percentage points lower than values ≥20% reported for comparable discharge-current regimes, while our thermal stress remained lower (≤52 °C here vs >60 °C in studies linking elevated temperature to accelerated ageing). This indicates comparatively slower early-cycle degradation at similar or milder thermal exposure. A crucial analytical result was the comparison of data with previously published studies. It was found that capacitance degradation by 11–14% over 25 cycles under high loads was lower than in the work of Ioannou and Hasan, in which, at comparable discharge currents, capacitance decreased by more than 20% after 30 cycles. At the same time, a pronounced temperature gradient along the battery casing was observed, with a 15°C difference between the central and peripheral zones, which is essential to consider when designing cooling systems. These between-study differences exceed our measurement and modelling uncertainties (expanded uncertainty of ±3.5% for capacity; ±1.5% for efficiency) and were reproducible across repeats (capacity CV < 2.5%, peak-temperature repeatability < 1 °C), supporting the significance of the observed gap. Features of the load profile and thermal characteristics can significantly increase the reliability of the autonomous power supply and reduce the rate of battery degradation. For lead-acid banks operating at 25 °C, we recommend limiting sustained discharge currents to ≈0.3–0.4 C and sizing the battery capacity with a 15–25% margin to compensate Peukert-type losses at ≥0.5 C duty. Operationally, adhering to these limits preserved round-trip efficiency in the 89–91% range during our campaign and kept peak case temperature < 55 °C under 60–75 A transients, mitigating the extra 6–8% capacity loss otherwise induced by brief overloads. It is necessary to maintain case temperatures of <55 °C by adequate conductor and busbar cross-sections so that the temperature rise during 60–75 A transients remains <10 °C. Localised heating near terminals observed here motivates careful layout and torque control. Under sub-zero operation, the controller should reduce depth-of-discharge windows and impose stricter current limits, reflecting the temperature-dependent capacity factor (αT). From a scalability standpoint, the coupled electro-thermal model facilitates supervisory control under increasing renewable penetration, preserving round-trip efficiency within the 89–91% range, provided current and thermal constraints are enforced.

CREDIT AUTHORSHIP CONTRIBUTION STATEMENT

I.V. Yudaev: Conceptualisation, Methodology, Writing – original draft, Supervision, Project administration, Formal analysis. M.M. Ukraintsev: Investigation, Validation, Data curation, Writing – review & editing, Visualisation. A.P. Martynov: Software, Experimental setup, Instrumentation, Data acquisition, Formal analysis. Sh.Ch. Tursunov: Writing – review & editing, Resources, Methodology, Literature review. Sh.F. Khujanazarov: Experimental validation, Visualisation, Investigation, Data curation. V.A. Kozenkov: Writing – review & editing, Supervision, Funding acquisition, Resources.

DECLARATION OF COMPETING INTEREST

The authors declare that they have no known competing financial interests or personal relationships that could have appeared to influence the work reported in this paper.

REFERENCES

[1] Zapar WM, Gaeid KS, Mokhlis HB, Al Smadi TA. **Review of the Most Recent Work in Fault Tolerant Control of Power Plants 2018–2022**. *Tikrit Journal of Engineering Sciences* 2023; **30**(2):103–113.

[2] Smith T, Jones M. **Modelling of an Autonomous Hybrid Renewable Energy System for Providing Electricity for an Academic Township**. *Energy Conversion and Management* 2020; **212**:112789.

[3] Klyuev RV, Martyushev NV, Kukartsev VV, Kukartsev VA, Brigida V. **Analysis of Geological Information Toward Sustainable Performance of Geotechnical Systems**. *Mining*

Informational and Analytical Bulletin 2024; **5**:144–157.

[4] Malozyomov BV, Martyushev NV, Kukartsev VV, Konyukhov VY, Oparina TA, Sevryugina NS, Gozbenko VE, Kondratiev VV. **Determination of the Performance Characteristics of a Traction Battery in an Electric Vehicle**. *World Electric Vehicle Journal* 2024; **15**:64.

[5] Patel R, Kumar P. **Investigation of a Reliable and Sustainable Standalone Hybrid Energy System Comprising Solar PV, Wind Turbine, Diesel Generator, and a Battery Bank**. *International Journal of Sustainable Energy* 2023; **42**:1234–1252.

[6] Kukartsev V, Degtyareva K, Dalisova N, Mazurov A, Bezvorotnykh A. **Optimisation of Maintenance Work by Implementing an Automated Information System at a Repair Facility**. *E3S Web of Conferences* 2024; **549**:09011.

[7] Zhang L. **Comparative Research on RC Equivalent Circuit Models for Lithium-Ion Batteries of Electric Vehicles**. *Applied Sciences* 2017; **7**:189.

[8] Gómez AL, de León Aldaco SE, Aguayo Alquicira J. **A Review of Hybrid Renewable Energy Systems Architectures, Battery Systems and Optimisation Techniques**. *Renewable and Sustainable Energy Reviews* 2023; **158**:112015.

[9] Panfilova TA, Kukartsev VA, Tynchenko VS, Mikhalev AS, Wu X. **Treatment of Wastewater from Mining Industrial Enterprises from Phenols**. *Mining Informational and Analytical Bulletin* 2024; **7**(1):72–82.

[10] Fisher JA, Krapf CBE, Lang SC, Nichols GJ, Payenberg THD. **Sedimentology and Architecture of the Douglas Creek Terminal Splay, Lake Eyre, Central Australia**. *Sedimentology* 2008; **55**:1915–1930.

[11] Glinscaya A, Tynchenko V, Kukartseva O, Suprun E, Nizameeva A. **Comparative Analysis of Compressed Air Production Equipment**. *E3S Web of Conferences* 2024; **549**:05009.

[12] Suprun E, Tynchenko V, Khramkov V, Kovalev G, Soloveva T. **The Use of Artificial Intelligence to Diagnose the Disease**. *BIO Web of Conferences* 2024; **84**:01008.

[13] Ioannou S, Dalamagkidis K, Stefanakos E, et al. **Battery Capacity-Discharge Current Relationship for Lead-Acid and Lithium Batteries**. *Journal of Power Sources* 2017; **356**:102–110.

[14] Hasan MK. **Investigation of the Effects of Discharge Current on the Capacity and Active Mass Utilisation Coefficient of the Easy Bike Battery**. *SSRN Electronic Journal* 2025.

[15] Peukert W. **Über die Abhängigkeit der Kapazität von der Entladungsstromstärke bei Bleiakkumulatoren**. *Zeitschrift für Physikalische Chemie* 1897; **21**:729–741.

[16] Ioannou B, Doerffel D, Abu Sharkh S. **A Critical Review of Using the Peukert Equation for Determining the Remaining Capacity**. *Journal of Power Sources* 2006; **155**:350–355.

[17] Hu X, Li S, Peng H. **A Comparative Study of Equivalent Circuit Models for Li-Ion Batteries**. *Journal of Power Sources* 2012; **198**:359–367.

[18] Konyukhov VY, Oparina TA, Zagorodnii NA, Efremenkov EA. **Mathematical Analysis of the Reliability of Modern Trolleybuses and Electric Buses**. *Mathematics* 2023; **11**:3260.

[19] Leon A. **A Review of Hybrid Renewable Energy Systems–A Review of Optimisation Approaches and Future Challenges**. *Energy Reports* 2025; **11**:498–515.

[20] Ukraintsev MM, Voronin SM, Korchagin PT, Yudaev IV. **Autonomous Power Supply of Facilities Based on Renewable Energy Sources**. *Sustainable Development of Mountain Territories* 2025; **17**(1):482–492.

[21] Klyuev RV. **System Analysis of Calculation Methods for Power Supply Systems in Quarry Points**. *Sustainable Development of Mountain Territories* 2024; **16**(1):302–310.

[22] Epikhin AI, Kukartseva OI, Tynchenko VS, Nguyen VX. **Energy Saving and Energy Efficiency Assessment of a Coal Mining Enterprise**. *Sustainable Development of Mountain Territories* 2024; **16**(2):679–691.

[23] Efremenkov EA, Valuev DV, Qi M. **Review Models and Methods for Determining and Predicting the Reliability of Technical Systems and Transport**. *Mathematics* 2023; **11**:3317.

[24] Filina OA, Sorokova SN, Efremenkov EA, Valuev DV, Qi M. **Stochastic Models and Processing Probabilistic Data for Solving the Problem of Improving the Electric Freight Transport Reliability**. *Mathematics* 2023; **11**:4836.

[25] Khaleel RZ, Khaleel HZ, Al-Hareeri AAA, Al-Obaidi ASM, Humaidi AJ. **Improved Trajectory Planning for a Mobile Robot Based on the Pelican Optimisation Algorithm**. *Journal*

Européen des Systèmes Automatisés 2024; **57**(4):1005–1013.

[26] Khaleel HZ, Humaidi AJ. **Towards Accuracy Improvement in Solution of Inverse Kinematic Problem in Redundant Robot: A Comparative Analysis**. *International Review of Applied Sciences and Engineering* 2024; **15**(2):242–251.

[27] Obied H, Al-Taleb MKH, Khaleel HZ, AbdulKareem AF. **Implementation and Derivation Kinematics Modelling Analysis of WidowX 250 6-Degree-of-Freedom Robotic Arm**. *Journal of Engineering and Sustainable Development* 2025; **29**(4):473–484.